Chain Unfolding Equilibria of α-Tropomyosin Coiled Coils Studied by Small Angle X-ray Scattering

Yoshio Muroga,*,† Tetsuya Muraki,† Ichiro Noda,† Hiroyuki Tagawa,‡ Alfred Holtzer,§ and Marilyn E. Holtzer§

Contribution from the School of Engineering, Nagoya University, Chikusa-ku, Nagoya, 464 Japan, and Department of Chemistry, Washington University, St. Louis, Missouri 63130

Received October 12, 1994[⊗]

Abstract: Scattering curves were obtained for α-tropomyosin two-stranded, coiled coils having the helix fraction ranging from 0.40 to 0.95 by small angle X-ray scattering with synchrotron orbital radiation. The observed curves were analyzed by comparison with the theoretical scattering function computed for two chain-conformational models: In model I, it is assumed that both ends of the helical protein unfold (fray) first as temperature is increased; in model II, it is assumed that the middle part unfolds first. The resulting theoretical functions are very different for the two models. Comparison with the observed curves, using a reasonable value for the effective bond length in the randomly-coiled state (12 Å), clearly shows that model I successfully mimicks the experiment whereas model II does not. This finding answers a long-standing question as to the location of the unfolded region in the tropomyosin molecule under conditions where it is still mostly dimeric and only somewhat unfolded.

Introduction

As is well-known, the native α-tropomyosin molecule comprises two 284-residue right-handed α-helical polypeptide chains set side-by-side in parallel and in register and given a slight, left-handed supertwist. In the absence of interchain cross-links, the double helix unfolds to two separated, randomly-coiled chains as the temperature is raised. This thermal transition provides a model for testing general concepts of protein folding and has been under experimental study for some time.[1] Since light-scattering experiments showed that the molecular weight of the protein decreases with a decrease in the helix content, Yukioka *et al.*[2] concluded that the dissociation of the two chains and the loss of helix occurs in the same general temperature domain; that is, the two processes may be closely coupled, as theory suggested earlier.[1]

Now, our interest is directed to another question: in the region of relatively low temperature, where dimers predominate, which part of the double-helical rod unfolds first as the temperature is raised? Some think it is around the middle of the rod, because of the presence of a vulnerable segment at residues ~130−190; others think that it is the ends that fray first. Needless to say, such a difference in the mode of chain unfolding should lead to different conformations that may be distinguishable by small angle X-ray scattering (SAXS). In earlier papers,[3−7] some of us showed experimentally and theoretically that a difference in local conformation of a polymer chain is clearly reflected in the particle-scattering curve in a comparatively high scattering vector range, as obtained by small angle X-ray scattering. Therefore, a difference in the conformation of the protein is expected to yield differences in the particle-scattering function, $P(\theta)$.

Although the two processes of chain dissociation and loss of the helix content proceed simultaneously, more or less, at any temperature, the temperature dependence[2] of the molecular weight shows that, below *ca.* 30−40 °C, dissociation of the two chains is negligible. The purpose of the present paper is to study which part of the double-helical, rodlike dimer unfolds first with temperature by comparing the observed scattering curves with the theoretical $P(\theta)$ for two typical models. Model I corresponds to the conformation realized when the molecule unfolds first by fraying at both ends of the double-helical rod, and model II, to the conformation realized when the implicated middle part unfolds first (Figure 1).

Materials and Methods

Preparation of α-tropomyosin from rabbit cardiac muscle and general manipulation of the protein are described in a previous paper.[2] Any disulfide bonds between the cysteines at position 190 in the protein chains were reduced with dithiothreitol (DTT) and protected from reoxidation by excess DTT. The solvent used was aqueous $(NaF)_{500}$-$(NaPi)_{50}(DTT)_{10}(7.4)$, denoted by giving the chemical formula of each solute in parentheses with its millimolarity as subscript, followed by the pH in parentheses. For SAXS experiments, NaF was employed in place of the more customary NaCl, because the incident X-ray beam is absorbed far less by the aqueous solution of NaF. Protein concentrations (C_p) were determined by using the absorbance at 277 nm with an extinction coefficient of 0.314 $cm^2\ mg^{-1}$.

The scattering curve of the protein molecule was measured by SAXS at C_p = 6.3 mg/mL. The temperature of the sample solution was successively set to 10, 20, 30, 40, and 50 ± 0.1 °C. The helix fraction (g) at these temperatures, determined from CD measurements,[1] was estimated to be 0.95, 0.92, 0.86, 0.78, and 0.40, respectively, neglecting possible differences between NaF and NaCl media. SAXS experiments were carried out using synchrotron orbital radiation as an X-ray source set up in the Photon Factory of the National Laboratory for High Energy Physics at Tsukuba, Japan. The wavelength of the X-ray was 1.488 Å, and the distance between the sample and the detector was 900 mm. The scattering intensity was detected by a position-sensitive proportional

† Nagoya University.

‡ Permanent address: Faculty of Science and Technology, Nihon University, Chiyoda-ku, Tokyo 101, Japan.

§ Washington University.

⊗ Abstract published in *Advance ACS Abstracts*, May 1, 1995.

(1) Holtzer, A.; Holtzer, M. E.; Skolnick, J. In *Protein Folding*; Gierasch, L. M., King, J., Eds.; AAAS Books: Washington, DC, 1990; pp 177−190.
(2) Yukioka, S.; Noda, I.; Nagasawa, M.; Holtzer, M. E.; Holtzer, A. *Macromolecules* **1985**, *18*, 1083−1086.
(3) Muroga, Y. *Macromolecules* **1988**, *21*, 2751−2755.
(4) Muroga, Y.; Tagawa, H.; Hiragi, Y.; Ueki, T.; Kataoka, M.; Izumi, Y.; Amemiya, Y. *Macromolecules* **1988**, *21*, 2756−2760.
(5) Muroga, Y. *Macromolecules* **1992**, *25*, 3385−3391.
(6) Muroga, Y. *Macromolecules* **1992**, *25*, 6063−6065.
(7) Muroga, Y. *Macromolecules* **1994**, *27*, 2951−2955.

0002-7863/95/1517-5622$09.00/0

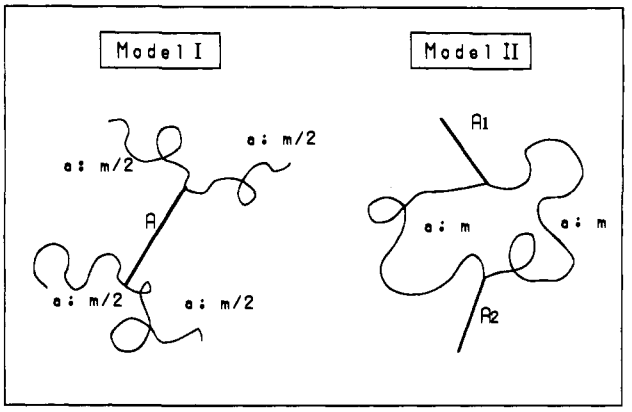

Figure 1. Two models for partially unfolded α-tropomyosin dimers. Model I corresponds to the conformation realized when both ends of the double-helical rod fray first and model II corresponds to the conformation realized when the middle part unfolds first, as temperature increases.

counter (PSPC) with 512 channels over 0.005−0.17 Å^{-1} in h, which is defined below as the magnitude of the scattering vector. The details of the instrumentation and the procedure are described elsewhere.[8] Effects of slit length and slit width on the scattering curves could be neglected, because the size of the X-ray beam at the sample position was small enough compared with the camera length. Scattered intensities were registered on a relative scale, not on an absolute scale. Therefore, the scattered intensities were multiplied by a constant factor for comparisons with theoretical curves.

Computation of the Scattering Function and the Mean-Square Radius for Models I and II

In general, the scattered intensity is proportional to R_θ, given by summation over all pairs of scattering points, j and k, in a molecule:

$$R_\theta = \sum_j \sum_k \exp[i\vec{\mathbf{h}}\cdot\vec{\mathbf{r}}_{jk}] \tag{1}$$

and the scattering function, $P(\theta)$, is defined by

$$P(\theta) = \frac{R_\theta}{\sum_j \sum_k 1} \tag{2}$$

wherein $\vec{\mathbf{h}}$ is the scattering vector, whose absolute value is given by

$$h = (4\pi/\tilde{\lambda}) \sin(\theta/2) \tag{3}$$

wherein θ is a scattering angle and $\tilde{\lambda}$ is the wavelength of the light in the solution.

As is shown in Figure 1, both models I and II consist of rod(s) (R region) and random coils (C region). In such a case, R_θ is given as a sum of $R_{\theta,\mathrm{RR}}$, $R_{\theta,\mathrm{CC}}$, and $R_{\theta,\mathrm{RC}}$, where $R_{\theta,\mathrm{RC}}$, for example, means the scattering intensity obtained when one scatterer is located in an R region and another in a C region. For a broken rodlike chain where several straight rods are alternatively joined by random-coil chains, we previously computed R_θ averaged over all possible conformations of the chain, $\langle R_\theta \rangle$.[3,5,6] A straightforward modification of those results gives $\langle R_\theta \rangle_{\mathrm{RR}}$, $\langle R_\theta \rangle_{\mathrm{CC}}$, and $\langle R_\theta \rangle_{\mathrm{RC}}$ for models I and II, except $\langle R_\theta \rangle_{\mathrm{CC}}$ for model II, which is treated below.

(8) Ueki, T.; Hiragi, Y.; Izumi, Y.; Tagawa, H.; Kataoka, M.; Muroga, Y.; Matsushita, T.; Amemiya, Y. *Photon Factory Activity Rep.* **1982/1983**, VI70−VI71.

(A) Model I. Model I is represented by a rod of length A joined by two random-coil chains at one end of the rod and also by two random-coil chains at the other end. Each random-coil chain consists of $m/2$ residues each having effective bond length a; i.e., the quantity a is the ratio of the root-mean-square end-to-end distance in the randomly-coiled state divided by the square root of the number of residues and is therefore independent of chain length (Figure 1). Free rotation is allowed between the rod and the neighboring segment in a random-coil chain. The components of $\langle R_\theta \rangle$ for model I, $\langle R_\theta \rangle_{\mathrm{I}}$, are given as follows:

$$\langle R_\theta \rangle_{\mathrm{I,RR}} = A^2\left\{2\Lambda(\beta) - \left(\frac{2}{\beta}\right)^2 \sin^2\left(\frac{\beta}{2}\right)\right\} \tag{4}$$

$$\beta = Ah \tag{5}$$

$$\Lambda(\beta) = (1/\beta)\int_0^\beta \left(\frac{\sin(t)}{t}\right) \mathrm{d}t \tag{6}$$

$$\langle R_\theta \rangle_{\mathrm{I,CC}} = 2ma^2 + 4m^2a^2\left(\frac{1}{w} - \frac{1 - \mathrm{e}^{-w}}{w^2}\right) + 8m^2a^2\frac{(1 - \mathrm{e}^{-w/2})^2\nu}{w^2} \tag{7}$$

$$w = \frac{m\alpha^2}{6} \tag{8}$$

$$\alpha = ah \tag{9}$$

$$\nu = \frac{\sin\beta}{\beta} \tag{10}$$

$$\langle R_\theta \rangle_{\mathrm{I,RC}} = 8maA\Lambda(\beta)\frac{(1 - \mathrm{e}^{-w/2})}{w} \tag{11}$$

Thus, $\langle R_\theta \rangle_{\mathrm{I}}$ is given by

$$\begin{aligned}\langle R_\theta \rangle_{\mathrm{I}} &= \langle R_\theta \rangle_{\mathrm{I,RR}} + \langle R_\theta \rangle_{\mathrm{I,CC}} + \langle R_\theta \rangle_{\mathrm{I,RC}} \\ &= A^2\left\{2\Lambda(\beta) - \left(\frac{2}{\beta}\right)^2 \sin^2\left(\frac{\beta}{2}\right)\right\} + 2ma^2 + \\ &\quad 4m^2a^2\left(\frac{1}{w} - \frac{1 - \mathrm{e}^{-w}}{w^2}\right) + 8m^2a^2\frac{(1 - \mathrm{e}^{-w/2})^2\nu}{w^2} + \\ &\quad 8maA\Lambda(\beta)\frac{(1 - \mathrm{e}^{-w/2})}{w}\end{aligned} \tag{12}$$

The mean-square radius of the molecule, $\langle R_g^2 \rangle$, can be derived from the expansion form of $P(\theta)$ in the region $\langle R_g^2 \rangle h^2 < 1$:

$$P(\theta) = 1 - \frac{h^2\langle R_g^2 \rangle}{3} + \ldots \tag{13}$$

From eqs 2, 12, and 13, $\langle R_g^2 \rangle$ for model I, $\langle R_g^2 \rangle_{\mathrm{I}}$, is given by

$$\langle R_g^2 \rangle_{\mathrm{I}} = \frac{f^2A^2}{12} + \frac{(1 - f)^2}{24}\left(5ma^2 - 4a^2 + \frac{a^2}{m} + 6A^2\right) + \frac{2f(1 - f)}{24}(3ma^2 + 4A^2 - 2a^2) \tag{14}$$

$$f = \frac{A}{2ma + A} \tag{15}$$

The model in which the molecule unfolds at only one end is not considered here, since it is known from studies of subsequences of tropomyosin that both ends are comparable in stability.[9]

(B) Model II. Model II is represented by two rods joined by two intervening random-coil chains, where one rod at the carboxyl end has length A_1, the other at the amino end has length A_2, and each random-coil chain comprises m amino acid residues of length a (Figure 1). Free rotation is allowed between the rod and the neighboring segment in a random-coil chain. Here, $\langle R_\theta \rangle_{II,CC}$ is equivalent to $\langle R_\theta \rangle$ for a ringlike random-coil chain consisting of $2m$ residues of effective bond length a. Thus, as was shown by Cassasa,[10] $\langle R_\theta \rangle_{II,CC}$ is given by

$$\langle R_\theta \rangle_{II,CC} = 4m^2a^2\left(\frac{2}{\xi}\right)\mathscr{D}\left(\frac{\xi}{2}\right) \tag{16}$$

where $\mathscr{D}(x)$ is a so-called Dawson integral[11]

$$\mathscr{D}(x) = e^{-x^2}\int_0^x e^{t^2}\,dt \tag{17}$$

and ξ is related to $\langle R_g^2 \rangle$ of the ringlike chain, $\langle R_g^2 \rangle_{ring}$:

$$\xi^2 = 2\langle R_g^2 \rangle_{ring} h^2 \tag{18}$$

$$\langle R_g^2 \rangle_{ring} = \frac{ma^2}{6} \tag{19}$$

Thus, the expression for $\langle R_\theta \rangle_{II}$ is

$$\langle R_\theta \rangle_{II} = A_1^2\left\{2\Lambda(\gamma_1) - \left(\frac{2}{\gamma_1}\right)^2 \sin^2\left(\frac{\gamma_1}{2}\right)\right\} + A_2^2\left\{2\Lambda(\gamma_2) - \left(\frac{2}{\gamma_2}\right)^2 \sin^2\left(\frac{\gamma_2}{2}\right)\right\} + 2A_1A_2\Lambda(\gamma_1)\Lambda(\gamma_2)e^{-w} + 4m^2a^2\left(\frac{2}{\xi}\right)\mathscr{D}\left(\frac{\xi}{2}\right) + 4ma\{A_1\Lambda(\gamma_1) + A_2\Lambda(\gamma_2)\}\frac{(1 - e^{-w})}{w} \tag{20}$$

$$\gamma_1 = A_1h \tag{21}$$

$$\gamma_2 = A_2h \tag{22}$$

$\langle R_g^2 \rangle$ for model II is given by

$$\langle R_g^2 \rangle_{II} = (1 - f)^2\frac{ma^2}{6} + 2f(1 - f)\left\{\frac{ma^2}{4} + \frac{(A_1^2 - A_1A_2 + A_2^2)}{6}\right\} + f^2\left\{\frac{(A_1 + A_2)^2}{12} - \frac{A_1^2A_2^2}{2(A_1 + A_2)^2} + \frac{A_1A_2ma^2}{(A_1 + A_2)^2}\right\} \tag{23}$$

where f is given by eq 15.

Results and Discussion

As is reviewed by Porod,[12] the scattering intensity of a rodlike particle of length L and the mean-square radius of a cross section, $\langle R_{cs}^2 \rangle$, can be separated into the axial factor I_{thin} and the cross-sectional factor, I_{cs}:

$$I = I_{thin}I_{cs} \tag{24}$$

It is worth emphasizing here that $\langle R_{cs}^2 \rangle^{1/2}$ measures a *cross-sectional* dimension of the particle rather than an overall dimension. Here, I_{thin} is approximated by $L\pi/h$ and, in the scattering vector region of $h^2\langle R_{cs}^2 \rangle < 1$, I_{cs} is proportional to $\exp\{-1/2\langle R_{cs}^2 \rangle h^2\}$. In this h region, therefore:[4]

$$I \propto \frac{1}{h}\exp\{-1/2\langle R_{cs}^2 \rangle h^2\} \tag{25}$$

and the plot of $\ln(I_{obs}h)$ *vs* h^2 forms a straight line whose slope yields $\langle R_{cs}^2 \rangle$.

Figure 2 shows the plot of $\ln(I_{obs}h)$ *vs* h^2 at 10 °C (diamonds), 20 °C (crosses), 30 °C (plusses), 40 °C (triangles), and 50 °C (circles). The observed points in a sufficiently high h region form a straight line, and the slope gives $\langle R_{cs}^2 \rangle^{1/2}$ values of 8.0, 8.0, 7.5, 7.3, and 6.5 Å, respectively. It is noted that an arrow on each curve designates the value of h^* where $h^{*2}\langle R_{cs}^2 \rangle = 1$. It is seen that the linear relation between $\ln(I_{obs}h)$ and h^2 holds well sufficiently far down from h^{*2}, at least as long as the temperature is not too high, to obtain a first approximation of $\langle R_{cs}^2 \rangle^{1/2}$. The latter value can then be refined by successive approximations in comparison with the experimental data. The success of the resulting fits is discussed below.

It has been shown that, when a polymer chain consists of both rods and random-coil chains, $\langle R_{cs}^2 \rangle$ is related to $\langle R_{cs}^2 \rangle$ for the rod and for the random-coil chain by[4]

$$\langle R_{cs}^2 \rangle = g\langle R_{cs}^2 \rangle_{rod} + (1 - g)\langle R_{cs}^2 \rangle_{coil} \tag{26}$$

The present $\langle R_{cs}^2 \rangle$ data evaluated at some g values well satisfy eq 26, as is shown in Figure 3. The intercept of the straight line at $g = 1.0$ gives $\langle R_{cs}^2 \rangle^{1/2}_{rod} = 8.0$ Å, which corresponds to a rod radius of $r = 11.3$ Å. The latter agrees well with the known value for coiled coils of $r = 10$ Å.[13]

To analyze a chain conformation by comparison of the observed scattering curve with the theoretical ones developed for models I and II having no cross section (eqs 12 and 20, respectively), it is necessary to reduce the observed scattering intensity to that obtained if the chain had no cross section, I_{thin}. Here, it is assumed that the scattering intensity from the protein molecule can also be separated into I_{thin} and I_{cs}. Then, using I_{cs} computed from $\langle R_{cs}^2 \rangle$, I_{thin} is derived from the relation of $I_{thin} = I_{obs}/I_{cs}$. The scattering points for I_{thin} thus obtained are shown in Figure 4A (10 °C), B (20 °C), C (30 °C), D (40 °C), and E (50 °C) in the form of a Kratky plot, *i.e.*, as $I_{thin}h^2$ *vs* h.

As is shown in the preceding section, we can specify the theoretical scattering curve for model I (eq 12) by assigning values to three parameters, *i.e.*, the length of the rod portion (A), the effective bond length of the random-coil portion (a), and the number of randomly coiled amino acid residues in each peptide chain (m). For model II (eq 20) we require values for four parameters: A_1, A_2, a, and m. Now, for A and m, we can utilize the data[13] that α-tropomyosin is 400 Å long and has 284 residues per peptide chain. For A_1, some propose[14-16] that it should be about $^{400}/_3$ Å long independently of the relevant temperature below 40 °C. This corresponds to unfolding in the region of residues ~130−190 and yields

$$A = 400g \tag{27}$$

$$A_1 = \frac{400}{3} \tag{28}$$

$$A_2 = A - A_1 \tag{29}$$

$$m = 284(1 - g) \tag{30}$$

Thus, only parameter a remains unknown for models I and II.

(9) Holtzer, M. E.; Holtzer, A. *Biopolymers* **1990**, *30*, 985−993.

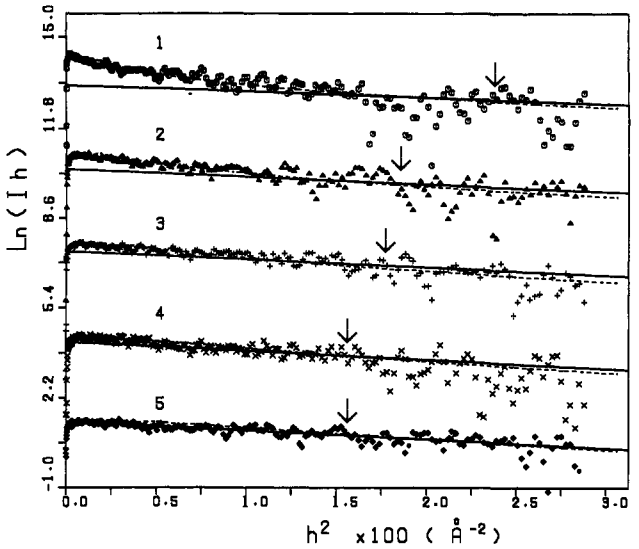

Figure 2. Plot of $\ln(I_{obs}h)$ *vs* h^2 to evaluate the mean-square radius of a cross section of the protein chain, $\langle R_{cs}^2 \rangle$, at 10 °C (diamonds), 20 °C (crosses), 30 °C (pluses), 40 °C (triangles), and 50 °C (circles). An arrow on each curve designates the value of h^* giving $h^{*2}\langle R_{cs}^2 \rangle = 1$. Dotted curves at 10, 20, 30, 40, and 50 °C curves are theoretical ones computed for model I using the helical fractions 0.95, 0.92, 0.86, 0.78, and 0.40, respectively, and assuming the effective bond length in the random-coiled state is 12 Å.

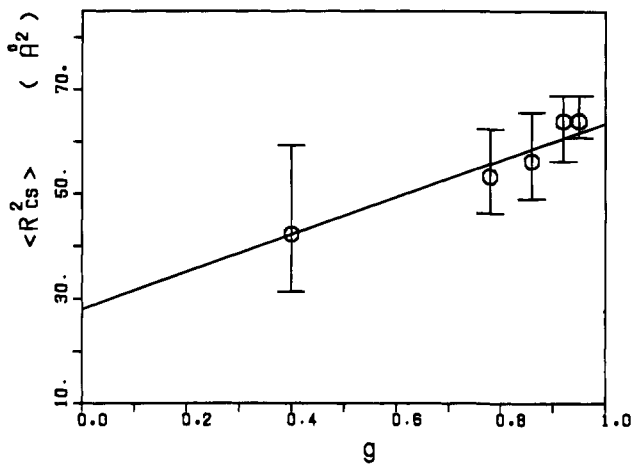

Figure 3. Helix fraction (g) dependence of the mean-square radius of a cross section of the protein chain, $\langle R_{cs}^2 \rangle$. Error estimates are shown by bars.

Here, in order to decide whether model I or II is more suitable to describe the conformation of α-tropomyosin in the early stages of the thermal transition, the data plots in Figure 2 and the Kratky plots (Figures 4A–E) are compared with the theoretical ones for model I (eq 12) and for model II (eq 20), computed with various values of a. It is clearly shown that both types of plot are satisfactorily reproduced by model I when a is within the range of *ca.* 8–14 Å whereas, as clearly seen from Figure 4, model II cannot reproduce the observed curves. Solid and dotted curves in the figure are for model I (best fit: $a = 12$ Å) and for model II with $a = 12$ Å, respectively. It is noteworthy that further calculations (not shown) indicate that the theoretical curves for model II are very insensitive to the values assumed for A_1 and A_2 as long as $A_1 + A_2$ (*i.e.* helix content) is kept constant.

The magnitude of a thus obtained from the fit to model I (12 Å) seems to be somewhat larger than the unperturbed value for random-coiled poly(L-glutamate), 8 Å, as evaluated from light scattering and viscosity.[17] This difference must be due to the excluded volume effect in the random-coiled state of α-tropomyosin. The expansion factor this implies, 1.38, is a bit smaller than that in poly(L-glutamate). This is not unexpected, since the protein contains some hydrophobic amino acids.

Since the properties of the isolated molecule are sought here, one must ask whether the concentration in our experiments is sufficiently low. The concentration of the solution (C_p^*) above which the solute molecules begin to overlap is estimated by[18]

$$C_p^* = \frac{M_w}{(4/3)\pi\langle R_g^2 \rangle^{3/2} A_v} \tag{31}$$

where M_w and A_v are the molecular weight of the native, two-stranded molecule (6.6×10^4) and Avogadro's number, respectively. Substituting $\langle R_g^2 \rangle$ for model I estimated by eq 14 into eq 31, C_p^* values at 10, 20, 30, 40, and 50 °C are roughly estimated to be 7.2, 6.6, 6.5, 7.5, and 22.2 mg/mL, respectively. Since the present sample concentration, 6.3 mg/mL, is near but below these values, it is expected that the scattering curve in a higher h region reflects the local conformation of an isolated two-chain molecule. Extant light-scattering experiments up to ~1 mg/mL indicate that solutions of α,α-tropomyosin under these conditions are free of aggregates of the native two-chain molecule.[2] The protein concentration employed in the SAXS experiments is a bit higher (~6 mg/mL), raising the question whether some aggregation may exist. However, we also have size exclusion HPLC data (not shown) indicating that, at the pH and ionic strength of the SAXS study, the mobility and homogeneity of the chromatograms are satisfactory and unaffectd by increasing the protein concentration up to 10 mg/mL. This combination of light scattering and size exclusion chromatography makes clear that the SAXS samples are molecularly dispersed. The concentration used here is comparable to the highest concentrations studied by CD.[1]

In conclusion, the scattering curves for α-tropomyosin obtained in the temperature range less than 40 °C, where the partially folded dimer predominates, support the suggestion that, in the thermal transition from the double-helix to two random-coil chains, the double helix unfolds first at the ends, not at the middle as temperature increases. This conclusion indicates that the entropy gain generated in the transition, which is significantly larger in model I than in model II, dominates over the demonstrated intrinsic structural weakness of residues 142–189, located near the center.[19]

These models are crude in that they do not take into account possible conformational heterogeneity in the equilibrium population.[1] It should be possible in future studies to examine the influence of such heterogeneity on the calculated $P(\theta)$ curves. However, in the region of interest here, wherein helix content is relatively high and dimers dominate, it is highly unlikely that this effect could alter the relative success of model I and failure of model II in mimicking the experimental results. The

(10) Cassasa, E. F. *J. Polym. Sci., Part A* **1965**, *3*, 605–614.
(11) In *Handbook of Mathematical Functions*; Abramowitz, M., Stegun, I. A., Eds.; Dover: New York, 1970; p 319.
(12) Porod, G. In *Small Angle X-ray Scattering*; Glatter, O., Kratky, O., Eds.; Academic Press: New York, 1982; pp 17–51.
(13) Fraser, R. D. B.; MacRae, T. P. In *Conformation in Fibrous Proteins*; Academic: New York, 1973; pp 419–468.
(14) Privalov, P. *Adv. Protein Chem.* **1982**, *35*, 1–104.
(15) Graceffa, P.; Lehrer, S. S. *J. Biol. Chem.* **1980**, *255*, 11296–11300.
(16) Graceffa, P.; Lehrer, S. S. *Biochemistry* **1984**, *23*, 2606–2612.
(17) Hawkins, R. B.; Holtzer, A. *Macromolecules* **1972**, *5*, 294–301.
(18) de Gennes, P. G. In *Scaling Concepts in Polymer Physics*; Cornell University Press: Ithaca, NY, 1979; p 76.
(19) Holtzer, M. E.; Crimmins, D. L.; Holtzer, A. *Biopolymers* **1995**, *35*, 125–136.

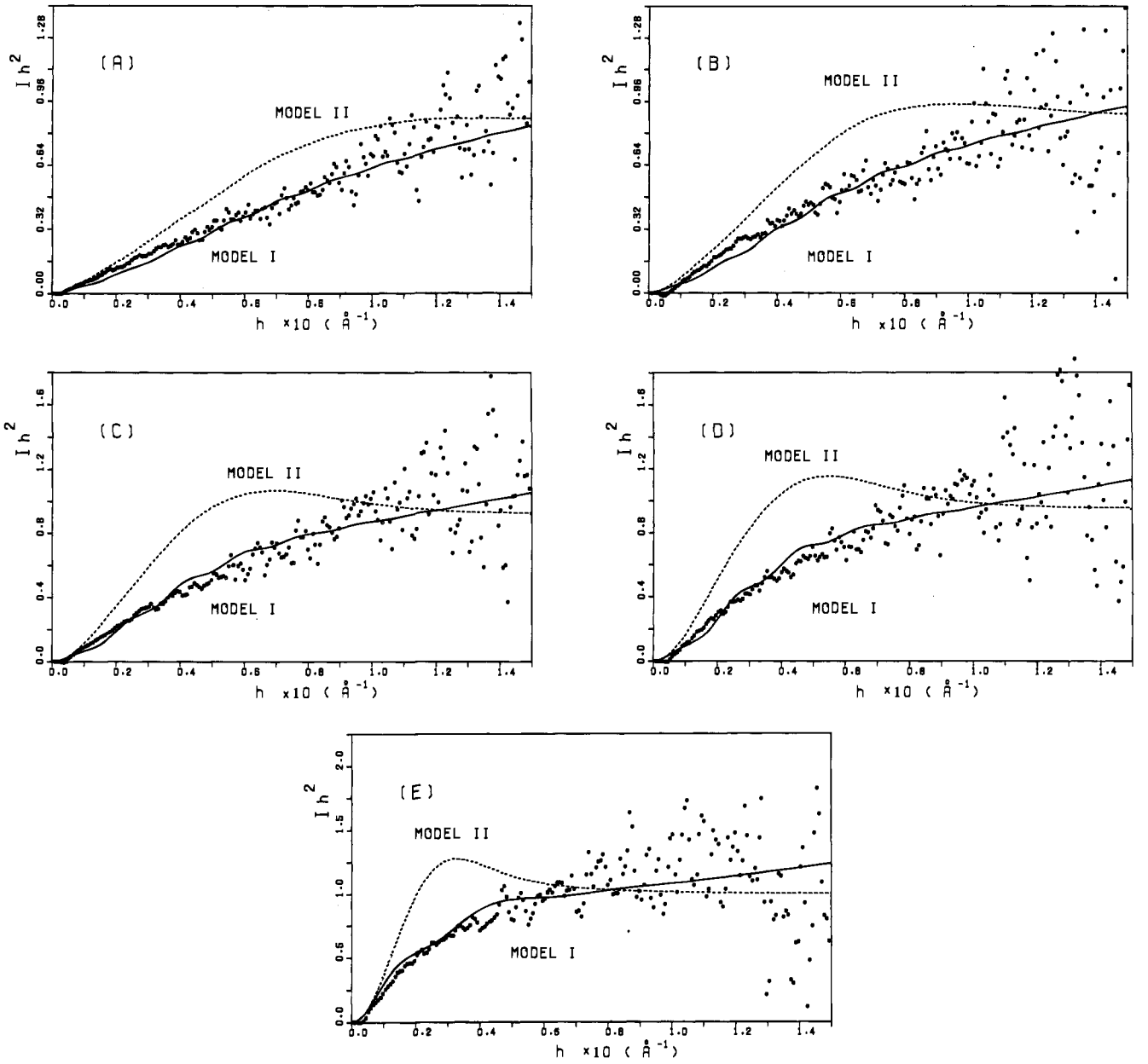

Figure 4. Comparison between the observed scattering (points) and the theoretical scattering functions for models I (solid curve) and II (dotted curve) at 10 °C (A), 20 °C (B), 30 °C (C), 40 °C (D), and 50 °C (E). The theoretical functions were computed using the helix fractions 0.95, 0.92, 0.86, 0.78, and 0.40, respectively, and assuming the effective bond length in the random-coiled state is 12 Å.

observed $P(\theta)$ in a scattering experiment is, in general, given by $\sum_i w_i M_i P_i(\theta)/M_w$, wherein w_i and $P_i(\theta)$ are the weight fraction and the particle-scattering factor of the ith conformational species, respectively, and M_w is the weight-averaged molecular weight.[20] In the present instance, the relevant regime is ≤40 °C, wherein only dimeric conformational states are appreciably populated.[2] The above expression for the observed $P(\theta)$ thus reduces to $\sum_i w_i P_i(\theta)$, a simple weight average of the individual particle-scattering factors. This simple averaging (the same as a number average here) cannot yield the experimentally observed curves of Figure 4A–D if an appreciable population of species is characterized by curves like the ones given by model II.

Acknowledgment. We are indebted to Professor M. Nagasawa of Toyota Technological Institute for valuable discussions. This work was supported in part by Grant No. GM-20064 from the Division of General Medical Sciences, United States Public Health Service, and in part by a grant from the Muscular Dystrophy Association.

JA943340R

(20) Zimm, B. H. *J. Chem. Phys.* **1948**, *16*, 1099–1116.